



**Development of hafnium metal and titanium-hafnium alloys  
having apatite-forming ability by chemical surface  
modification**

Journal:	<i>Journal of Biomedical Materials Research: Part B - Applied Biomaterials</i>
Manuscript ID	JBMR-B-17-0566.R2
Wiley - Manuscript type:	Original Research Report
Date Submitted by the Author:	n/a
Complete List of Authors:	Miyazaki, Toshiki; Kyushu Institute of Technology, Graduate School of Life Science and Systems Engineering Sueoka, Masaya; Kyushu Institute of Technology, Graduate School of Life Science and Systems Engineering Shirosaki, Yuki; Kyushu Institute of Technology Shinozaki, Nobuya; Kyushu Institute of Technology Shiraishi, Takanobu; Nagasaki University, Dental and Biomedical Materials Science
Keywords:	Hafnium, Titanium-hafnium alloy, Bone-bonding, Surface treatment, Apatite

SCHOLARONE™  
Manuscripts

This is the peer reviewed version of the following article: <https://onlinelibrary.wiley.com/doi/abs/10.1002/jbm.b.34068>, which has been published in final form at <https://doi.org/10.1002/jbm.b.34068>. This article may be used for non-commercial purposes in accordance with Wiley Terms and Conditions for Self-Archiving.

1  
2  
3  
4  
5  
6 **Development of hafnium metal and titanium-hafnium alloys having**  
7 **apatite-forming ability by chemical surface modification**  
8  
9

10  
11  
12 Toshiki Miyazaki<sup>a,\*</sup>, Masaya Sueoka<sup>a</sup>, Yuki Shirosaki<sup>b</sup>, Nobuya Shinozaki<sup>a</sup> and  
13  
14 Takanobu Shiraishi<sup>c</sup>  
15  
16

17  
18  
19 <sup>a</sup>Graduate School of Life Science and System Engineering, Kyushu Institute of  
20  
21 Technology, Kitakyushu, Japan  
22  
23

24 <sup>b</sup>Graduate School of Engineering, Kyushu Institute of Technology, Kitakyushu, Japan  
25

26 <sup>c</sup>Graduate School of Biomedical Sciences, Nagasaki University, Nagasaki, Japan  
27  
28  
29

30  
31 Corresponding author:  
32

33 Toshiki Miyazaki  
34

35  
36 Graduate School of Life Science and Systems Engineering, Kyushu Institute of  
37  
38 Technology, 2-4, Hibikino, Wakamatsu-ku, Kitakyushu 808-0196, Japan  
39  
40

41 Tel/Fax: +81-93-695-6025  
42

43 E-mail: tmiya@life.kyutech.ac.jp  
44  
45  
46  
47  
48  
49  
50  
51  
52  
53  
54  
55  
56  
57  
58  
59  
60

**Abstract**

Hafnium (Hf) has attracted considerable attention as a component of biomedical titanium (Ti) alloys with low Young's moduli and/or shape-memory functionalities, because its cytotoxicity is as low as that of Ti. The drawback of metals is that their bone-bonding ability is generally low. It is known that apatite formation in the body is a prerequisite for bone-bonding. Although several chemical treatments have been proposed for preparing Ti for bone-bonding, there have been no similar investigations for Hf. In the present study, NaOH- and heat-treatments were applied to pure Hf and Ti-Hf alloys and their bone-bonding ability was assessed *in vitro* with the use of simulated body fluid (SBF). After NaOH- and heat-treatments, anatase formed on alloys with low Hf content (20–40% (atom%) Hf); mixtures of sodium titanate and hafnium titanate formed on alloys with similar Ti and Hf content (60% Hf); and hafnium oxide formed on alloys with high Hf content (80% Hf and pure Hf). Precipitates of apatite were observed on all the metals in SBF, except for the alloy with 60% Hf. We speculated that the hafnium titanate formed on this alloy had a low apatite-forming ability owing to its high negative surface charge, which inhibited P adsorption. The apatite-forming abilities of the Ti-Hf alloys strongly

1  
2  
3  
4  
5  
6 depended on their Hf content. The present results indicate that Hf-based materials have  
7  
8  
9 good potential for bone-bonding.  
10  
11  
12  
13  
14

15 **Keywords:** Hafnium, Titanium-hafnium alloy, Bone-bonding, Surface treatment,  
16  
17  
18 Apatite  
19  
20  
21  
22  
23  
24  
25  
26  
27  
28  
29  
30  
31  
32  
33  
34  
35  
36  
37  
38  
39  
40  
41  
42  
43  
44  
45  
46  
47  
48  
49  
50  
51  
52  
53  
54  
55  
56  
57  
58  
59  
60

For Peer Review

## 1. Introduction

Hafnium (Hf) belongs to the same group of elements as titanium (Ti) and zirconium (Zr), which are applied for clinical replacement of hard tissue and have similar chemical properties. It is known that the cytotoxicity of hafnium is as low as that of Ti and Zr [1]. Recently, addition of Hf to Ti has been found to reduce the Young's modulus of the resulting alloy from 120 to 110 GPa [2,3]. In addition, Hf has attracted considerable attention as a component of nickel-free shape memory alloys for medical applications [4].

However, many metallic materials do not bond with bone easily and this property must be improved to enable their application to hard tissue reconstruction. An essential requirement for artificial materials to exhibit bone-bonding in the body is the formation of a bone-like apatite layer [5]. Chemical treatments based on aqueous solutions of sodium hydroxide (NaOH) [6] or hydrogen peroxide [7], followed by heat treatments, and anodic oxidation [8] are known to be effective techniques for enhancing the apatite-forming ability on Ti metal surfaces. Tantalum (Ta) [9] and Zr [10] can also exhibit bone-bonding properties following NaOH treatments. However, the effects of such surface treatments on Hf remain unclear.

1  
2  
3  
4  
5  
6 In this study, pure Hf metal and Ti-Hf alloys were subjected to NaOH- and  
7  
8  
9 heat-treatments and the apatite-forming abilities of the treated alloys were investigated in  
10  
11  
12 simulated body fluid (SBF). Differences in the apatite-forming ability are discussed in  
13  
14  
15 terms of the components of the alloy and the crystalline phase of the surface after the  
16  
17  
18 treatments.  
19

## 20 21 22 23 24 **2. Materials and methods**

### 25 26 27 **2.1. Materials**

28  
29  
30 NaOH and the reagents used to prepare SBF were purchased from Nacalai Tesque  
31  
32  
33 Inc., Kyoto, Japan, hafnium oxide (HfO<sub>2</sub>) from Kojundo Chemical Laboratory Co., Ltd.  
34  
35  
36 Saitama, Japan, and anatase from Ishihara Sangyo Kaisha, Ltd., Osaka, Japan.  
37  
38  
39

### 40 41 42 **2.2. NaOH- and heat-treatments**

43  
44  
45  
46 Pure Hf substrates (Nilaco Co., Tokyo, Japan)  $10 \times 10 \times 0.1 \text{ mm}^3$  in size and Ti-Hf  
47  
48  
49 alloy substrates (Kindly prepared by arc melting in Institute for Materials Research,  
50  
51  
52 Tohoku University, Sendai, Japan)  $5 \times 5 \times 7 \text{ mm}^3$  in size were polished with #500 SiC  
53  
54  
55

1  
2  
3  
4  
5  
6 paper. Ti-Hf alloy containing x atom% of Hf is hereafter denoted as Ti-xHf. Each  
7  
8  
9 substrate was then soaked in 5 mL of 10 M-NaOH aqueous solution and mechanically  
10  
11  
12 agitated in a water bath (H-10, Taitec Co., Saitama, Japan) at 60 °C for 1 day. The  
13  
14  
15 agitating speed was fixed at 120 strokes/min. The substrates were then removed from  
16  
17  
18 solution, gently washed with ultrapure water, and dried at 60°C. The substrates were  
19  
20  
21 then heated to 400°C at 5 °C/min, maintained at 400°C for 1 h, and allowed to cool to  
22  
23  
24 room temperature in the furnace.  
25

26  
27  
28 Hafnium oxide and hafnium titanate (HfTiO<sub>4</sub>) powders were used for zeta potential  
29  
30  
31 measurements as model compounds for the surface crystal phase of the chemically  
32  
33  
34 treated metals. The HfO<sub>2</sub> reagent was used as received. HfTiO<sub>4</sub> was prepared by  
35  
36  
37 calcinating a mixture of HfO<sub>2</sub> and anatase at a molar ratio of 1:1 at 1300°C for 5 h.  
38  
39  
40 X-ray diffraction measurements confirmed that the obtained powder consisted of a  
41  
42  
43 single phase of HfTiO<sub>4</sub> (JCPDS#40-794).  
44  
45

### 46 47 48 49 2.3. Soaking in SBF

50  
51  
52  
53 The treated substrates were soaked in 30 mL of SBF containing the following  
54  
55  
56  
57  
58  
59  
60

1  
2  
3  
4  
5  
6 inorganic ion concentrations (142.0 mM Na<sup>+</sup>, 5.0 mM K<sup>+</sup>, 1.5 mM Mg<sup>2+</sup>, 2.5 mM Ca<sup>2+</sup>,  
7  
8  
9 147.8 mM Cl<sup>-</sup>, 4.2 mM HCO<sub>3</sub><sup>-</sup>, 1.0 mM HPO<sub>4</sub><sup>2-</sup>, and 0.5 mM SO<sub>4</sub><sup>2-</sup>) at 36.5 °C for  
10  
11  
12 various periods. The pH of the solution was buffered at 7.40 by 50 mM  
13  
14  
15 tris(hydroxymethyl)aminomethane and an appropriate amount of HCl. SBF was  
16  
17  
18 prepared according to the literature [11]. After soaking, the substrates were removed  
19  
20  
21 from the SBF and then immersed in ultrapure water for 30 min to remove excess  
22  
23  
24  
25 water-soluble salts on their surfaces.  
26  
27  
28  
29  
30

#### 31 2.4. Characterization 32 33

34 The surface structural changes of the substrates were characterized by scanning  
35  
36  
37 electron microscope imaging (SEM; Model S-3500N; Hitachi Co., Tokyo, Japan),  
38  
39  
40 energy dispersive X-ray spectroscopy (EDX; Model EX-400; Horiba Co., Kyoto, Japan),  
41  
42  
43 thin-film X-ray diffraction (TF-XRD; MXP3V; Mac Science Ltd., Yokohama, Japan),  
44  
45  
46 X-ray photoelectron spectroscopy (XPS, KRATOS AXIS-Nova, Shimadzu Co., Kyoto,  
47  
48  
49 Japan) and Fourier-transform infrared spectroscopy (FT-IR, FT/IR-6100, JASCO Co.,  
50  
51  
52 Tokyo, Japan). Zeta potentials of the powder in 10 mM NaCl were measured with a  
53  
54  
55  
56  
57  
58  
59  
60

1  
2  
3  
4  
5  
6 zeta-potential analyzer (ELS-Z, Otsuka Electronics Co., Osaka, Japan) in a connected  
7  
8  
9 box-like quartz cell. The obtained zeta potential was statistically analyzed by t-test.  
10

11  
12 In TF-XRD experiments, the incident beam was fixed at  $1^\circ$  to the surface of each  
13  
14 substrate, at a scan rate of  $0.02^\circ \cdot \text{s}^{-1}$ . In XPS experiments, the measured binding energies  
15  
16 were corrected against the C1s binding energy of hydrocarbon methylene groups (284.6  
17  
18 eV) adsorbed on the substrate surface. In FT-IR measurements, an attenuated total  
19  
20 reflection (ATR) attachment with a diamond crystal was used.  
21  
22  
23  
24  
25  
26  
27  
28  
29  
30

### 31 **3. Results**

32  
33  
34 Fig. 1 shows XPS spectra of NaOH- and heat-treated metal substrates. Peaks at 530 eV  
35  
36 are assigned to M-O (M: Ti, Hf), those at 531 eV to acidic M-OH or physically adsorbed  
37  
38 water, and those at 532.5 eV to basic M-OH or chemically adsorbed water [12]. The  
39  
40 proportion of the peak attributed to basic M-OH groups or chemically adsorbed water  
41  
42 increased as the Ti content in the alloy increased. This result indicates that the NaOH- and  
43  
44 heat-treatments induced the largest proportion of M-OH groups on the surface of the  
45  
46 alloys with high Ti content.  
47  
48  
49  
50  
51  
52  
53  
54  
55  
56  
57  
58  
59  
60

1  
2  
3  
4  
5  
6 Fig. 2 shows TF-XRD patterns of the NaOH- and heat-treated metal substrates before  
7  
8  
9 and after immersion in SBF for 7 days. Peaks assigned to the  $\alpha'$  phase of Ti-Hf with a  
10  
11  
12 hexagonal close-packed structure shifted to a lower diffraction angle as the Hf content in  
13  
14  
15 increased in the alloy. Peaks assigned to anatase (JCPDS#21-1272) were observed for  
16  
17  
18 Ti-20Hf and Ti-40Hf; peaks assigned to  $\text{Na}_2\text{Ti}_5\text{O}_{11}$  (JCPDS#11-289) and  $\text{HfTiO}_4$   
19  
20  
21 (JCPDS#40-794) were found in Ti-60Hf; peaks assigned to  $\text{HfO}_2$  (JCPDS#34-104) were  
22  
23  
24 found in Ti-80Hf and Hf. Such crystalline phase was not observed except base metal just  
25  
26  
27 after NaOH treatment (data not shown), meaning that the above oxides were formed by  
28  
29  
30 the heating. The crystalline phases remained almost the same even after immersion in  
31  
32  
33 SBF.  
34  
35

36  
37 Fig. 3 shows SEM images and EDX spectra of the NaOH- and heat-treated metal  
38  
39  
40 substrates after immersion in SBF for 7 days. Formation of spherical particles was  
41  
42  
43 observed on the surfaces of the alloys except for the Ti-60Hf substrate. The particles were  
44  
45  
46 confirmed to contain a high proportion of Ca and P by EDX.  
47  
48  
49

50 Fig. 4 shows a high-magnification SEM image and FT-IR ATR spectrum of the  
51  
52  
53 spherical particles formed on the surface-treated Ti-80Hf after immersion in SBF for 7  
54  
55  
56  
57  
58  
59  
60

1  
2  
3  
4  
5  
6 days. A fine network morphology was observed, which was similar to that of the  
7  
8  
9 bone-like apatite formed in SBF [13]. In the FT-IR ATR spectrum, peaks assigned to  
10  
11  
12  $\text{PO}_4^{3-}$ ,  $\text{HPO}_4^{2-}$  and  $\text{CO}_3^{2-}$  were observed [14,15]. The peak of  $\text{HPO}_4^{2-}$  and  $\text{CO}_3^{2-}$  around  
13  
14  
15  $870\text{ cm}^{-1}$  was too close to distinguish from each other. The splitting of the  $\text{PO}_4^{3-}$  peaks at  
16  
17  
18  $600$  and  $1000\text{ cm}^{-1}$  is characteristic of apatite, and the presence of  $\text{CO}_3^{2-}$  suggested the  
19  
20  
21 formation of carbonate-containing non-stoichiometric apatite in SBF [16]. Therefore, the  
22  
23  
24 spherical particles in Fig. 3 are considered to be bone-like apatite.  
25

26  
27  
28 Table 1 shows the zeta potentials of  $\text{HfO}_2$  and  $\text{HfTiO}_4$ , indicating that  $\text{HfTiO}_4$  had a  
29  
30  
31 more negative surface charge than that of  $\text{HfO}_2$ .  
32

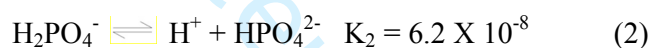
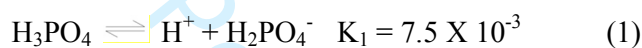
#### 33 34 35 36 37 **4. Discussion** 38

39  
40 We found that NaOH- and heat-treated Hf metal formed apatite on their surfaces in SBF.  
41  
42  
43 This result confirms that the Hf-OH group can act as a functional group that enables  
44  
45  
46 apatite formation, as previously reported for Si-OH and Ti-OH groups.  
47  
48

49  
50 The calcium phosphate precipitates formed on the substrates could not be identified  
51  
52  
53 as an apatite phase by TF-XRD, likely because of the small amount present. However, it  
54  
55  
56  
57

1  
2  
3  
4  
5  
6 has been reported that pure Ti treated with 5 M-NaOH and heated at 400°C forms  
7  
8  
9 apatite over its whole surface in SBF within 7 days [17]. Therefore, we observe that the  
10  
11  
12 apatite-forming ability of the Ti-Hf alloy and Hf metal is lower than that of pure Ti.  
13  
14  
15 There are two possible reasons for this result: First, the apatite-forming ability of  
16  
17  
18 Hf-OH itself is lower than that of Ti-OH. Second, Ti has a higher corrosion rate (5.0  
19  
20  
21 mm / year in 40% NaOH at 121°C) in NaOH solution than that of Hf (0.15 mm / year in  
22  
23  
24 38% NaOH at 115°C) [18,19]. Therefore, it is likely that fewer Hf-OH groups were  
25  
26  
27 formed by the NaOH- and heat-treatments, in spite that we used more concentrated  
28  
29  
30 NaOH (10 M) than previous research on surface treatment of Ti (5 M) [17]. This  
31  
32  
33 assumption is supported by our XPS spectra, which showed a low proportion of OH  
34  
35  
36 groups on the treated metals with high Hf content in Fig. 1. It is reported that a lot of  
37  
38  
39  $\text{Na}_2\text{Ti}_5\text{O}_{11}$  was mainly formed on Ti metal after 5 M-NaOH treatment and subsequent  
40  
41  
42 heating at 600°C [17], while amount of  $\text{Na}_2\text{Ti}_5\text{O}_{11}$  formed on the treated Ti-Hf alloy was  
43  
44  
45 very low (See Fig. 2). Therefore, this may also lead to low apatite formation on the  
46  
47  
48 present specimens in SBF. Chemical treatment of Hf metal with a more concentrated  
49  
50  
51 NaOH solution might be necessary in future studies.  
52  
53  
54  
55  
56  
57  
58  
59  
60

1  
2  
3  
4  
5  
6 It is noted that the formed apatite contained  $\text{HPO}_4^{2-}$  (See Fig. 4). Although Kokubo *et*  
7  
8  
9 *al.* developed bone-bonding Ti by 5 M-NaOH treatment and subsequent heat treatment at  
10  
11  
12 600°C, the apatite layer formed in SBF has not been characterized by FT-IR. On the other  
13  
14  
15 hand, other groups have reported that  $\text{HPO}_4^{2-}$ -containing apatite is detected on Ti and its  
16  
17  
18 alloys treated with 10 M-NaOH and heated at 600°C after soaking in SBF [20,21]. Acidic  
19  
20  
21 dissociation of phosphoric acid is described as follows:  
22



23  
24  
25  
26  
27  
28  
29  
30  
31  
32  
33  
34 It is assumed that approximately 60% of phosphate species takes a form of  $\text{HPO}_4^{2-}$  at  
35  
36  
37 pH7.40 based on these equilibria. Therefore, ion exchange would occur between  $\text{HPO}_4^{2-}$   
38  
39  
40 in SBF and  $\text{CO}_3^{2-}$  in the apatite crystals which are equivalent anion.  
41  
42

43  
44 Apatite was not formed on the Ti-60Hf, with an intermediate composition. The  
45  
46  
47 proportion of OH groups on the surface of this substrate was similar to those of Ti-80Hf  
48  
49  
50 and pure Hf, which both promoted apatite formation (See Fig. 1). Therefore, the low  
51  
52  
53 proportion of OH groups was unlikely to be the reason for the lack of apatite formation.  
54  
55  
56  
57  
58  
59  
60

1  
2  
3  
4  
5  
6 Our zeta potential measurements indicated that the surface of HfTiO<sub>4</sub> was highly  
7  
8  
9 negatively charged (see Table 1). The surface charge was much lower than that of Ti  
10  
11  
12 metal subjected to the NaOH- and heat-treatments (approximately -10 mV), which  
13  
14  
15 formed apatite [22]. Apatite nucleation on negatively charged materials such as NaOH-  
16  
17  
18 and heat-treated Ti and Ta, and Na<sub>2</sub>O-SiO<sub>2</sub> glass is triggered by initial Ca<sup>2+</sup> adsorption  
19  
20  
21 followed by PO<sub>4</sub><sup>3-</sup> adsorption [23,24,25]. Although Ca and P were detected on Ti-60Hf,  
22  
23  
24 the amounts were smaller than those of the other samples (see Fig. 3). Hence, we  
25  
26  
27 assume that the negative surface charge was neutralized by Ca<sup>2+</sup> adsorption onto HfTiO<sub>4</sub>  
28  
29  
30 but further PO<sub>4</sub><sup>3-</sup> adsorption was limited.  
31  
32  
33  
34  
35  
36

## 37 **5. Conclusion**

38  
39  
40 In this study, the apatite-forming abilities of pure Hf and Ti-Hf alloys subjected to  
41  
42  
43 NaOH- and heat-treatments were investigated in SBF. The following points were  
44  
45  
46 clarified.  
47  
48  
49

50 (1) Pure Hf metal subjected to the treatments enabled formation of apatite on its surfaces.

51  
52  
53 Therefore, Hf is a candidate metallic material, which exhibits bone-bonding potential.  
54  
55  
56  
57

1  
2  
3  
4  
5  
6 (2) The apatite-forming ability of Ti-Hf alloys was low at intermediate compositions.  
7  
8

9 Namely, apatite formation was not observed in Ti-60Hf. We speculate that highly  
10  
11  
12 negatively charged  $\text{HfTiO}_4$  inhibited  $\text{PO}_4^{3-}$  adsorption.  
13  
14  
15  
16  
17

### 18 **Acknowledgments**

19  
20  
21 The authors thank Ms. Akiko Nomura and Mr. Kazuo Obara of Institute for Materials  
22  
23  
24 Research, Tohoku University, Sendai, Japan for their contribution to sample alloy  
25  
26  
27 preparation.  
28  
29  
30  
31  
32  
33

### 34 **References**

- 35  
36  
37 1. Yamamoto A, Honma R, Sumita M. Cytotoxicity evaluation of 43 metal salts using  
38  
39  
40 murine fibroblasts and osteoblastic cells. *J Biomed Mater Res* 1998;39:331-340.  
41  
42  
43 2. Zhou YL, Niinomi M, Akahori T. Dynamic Young's Modulus and Mechanical  
44  
45  
46 Properties of Ti-Hf Alloys. *Mater Trans* 2004;45:1549-1554.  
47  
48  
49 3. Shiraishi T, Shishido T, Shinozaki N, Fujita T. The effects of Hf addition to Ti on  
50  
51  
52 its elastic modulus and corrosion resistance. *J Jpn Soc Dent Mater Devices*  
53  
54  
55  
56  
57

- 1  
2  
3  
4  
5  
6 2010;29:153 (in Japanese).  
7  
8  
9 4. Wang BL, Li L, Zheng YF. In vitro cytotoxicity and emocompatibility studies of  
10  
11 Ti-Nb,Ti-Nb-Zr and Ti-Nb-Hf biomedical shape memory alloys. Biomed Mater  
12  
13 2010;5:044102.  
14  
15  
16  
17  
18 5. Kokubo T, Kim HM, Kawashita M. Novel bioactive materials with different  
19  
20 mechanical properties. Biomaterials 2003;24:2161-2175.  
21  
22  
23  
24 6. Kim HM, Miyaji F, Kokubo T, Nakamura T. Preparation of bioactive Ti and its  
25  
26 alloys via simple chemical surface treatment. J Biomed Mater Res  
27  
28 1996;32:409-417.  
29  
30  
31  
32  
33  
34 7. Wang XX, Hayakawa S, Tsuru K, Osaka A. A comparative study of in vitro apatite  
35  
36 deposition on heat-, H<sub>2</sub>O<sub>2</sub>-, and NaOH-treated titanium surfaces. J Biomed Mater  
37  
38 Res 2001;54:172-178.  
39  
40  
41  
42  
43 8. Yang BC, Uchida M, Kim HM, Zhang X, Kokubo T. Preparation of bioactive  
44  
45 titanium metal via anodic oxidation treatment. Biomaterials 2004;25:1003–1010.  
46  
47  
48  
49 9. Miyazaki T, Kim HM, Miyaji F, Kokubo T, Nakamura T. Bioactive Tantalum Metal  
50  
51 Prepared by NaOH Treatment. J Biomed Mater Res 2000;50:35-42.  
52  
53  
54  
55  
56  
57  
58  
59  
60

- 1  
2  
3  
4  
5  
6 10. Uchida M, Kim HM, Miyaji F, Kokubo T, Nakamura T. Apatite formation on  
7  
8 zirconium metal treated with aqueous NaOH. *Biomaterials* 2002;23:313-317.  
9  
10  
11  
12 11. Cho SB, Kokubo T, Nakanishi K, Soga N, Ohtsuki C, Nakamura T, Kitsugi T,  
13  
14 Yamamuro T. Dependence of Apatite Formation on Silica Gel on Its Structure:  
15  
16 Effect of Heat Treatment. *J Am Ceram Soc* 1995;78:1769-1774.  
17  
18  
19  
20  
21 12. Nakao Y, Sugino A, Tsuru K, Uetsuki K, Shirosaki Y, Hayakawa S, Osaka A.  
22  
23 Enhancement of apatite-forming ability of parallelly aligned Ti-substrates with  
24  
25 optimum gaps by autoclaving. *J Ceram Soc Japan* 2010;118:483-486.  
26  
27  
28  
29  
30  
31 13. Kokubo T, Ito S, Huang ZT, Hayashi T, Sakka S, Kitsugi T, Yamamuro T.  
32  
33 Ca,P-rich layer formed on high-strength bioactive glass-ceramic A-W. *J. Biomed.*  
34  
35  
36  
37 Mater. Res. 1990;24:331-343.  
38  
39  
40  
41 14. Kandori K, Horigami N, Yasukawa A, Ishikawa T. Texture and Formation  
42  
43 Mechanism of Fibrous Calcium Hydroxyapatite Particles Prepared by  
44  
45  
46 Decomposition of Calcium-EDTA Chelates. *J Am Ceram Soc* 1997;80:1157-1164.  
47  
48  
49  
50 15. Drouet C. Apatite Formation: Why It May Not Work as Planned, and How to  
51  
52  
53 Conclusively Identify Apatite Compounds. *Biomed Res Int* 2013;2013:Article ID  
54  
55  
56  
57  
58  
59  
60

- 1  
2  
3  
4  
5  
6 490946.  
7  
8  
9 16. Kim HM, Kishimoto K, Miyaji F, Kokubo T, Yao T, Suetsugu Y, Tanaka J,  
10  
11 Nakamura T. Composition and structure of apatite formed on organic polymer in  
12  
13 simulated body fluid with a high content of carbonate ion. *J Mater Sci Mater Med*  
14  
15  
16  
17  
18 2000;11:421–426.  
19  
20  
21 17. Kim HM, Miyaji F, Kokubo T, Nakamura T. Effect of Heat Treatment on  
22  
23 Apatite-forming Ability of Ti Metal Induced by Alkali Treatment. *J Mater Sci*  
24  
25  
26  
27  
28  
29 Mater Med 1997;8:341-347.  
30  
31 18. Corrosion Resistance of Titanium. TIMET Corporation Brochure Denver:1997:18.  
32  
33  
34 19. Holmes DR. Corrosion of Hafnium and Hafnium Alloys. *ASM Handbook, Volume*  
35  
36  
37 13B, Corrosion: Materials. OH:ASM International;2005:354-359.  
38  
39  
40 20. Lin FH, Hsu YS, Lin SH, Chen TM. The growth of hydroxyapatite on alkaline  
41  
42  
43 treated Ti–6Al–4V soaking in higher temperature with concentrated  $\text{Ca}^{2+}/\text{HPO}_4^{2-}$   
44  
45  
46  
47 simulated body fluid. *Mater Chem Phys* 2004;87:24-30.  
48  
49  
50 21. Müller L, Müller FA. Preparation of SBF with different  $\text{HCO}_3^-$  content and its  
51  
52  
53 influence on the composition of biomimetic apatites. *Acta Biomater*  
54  
55  
56  
57  
58  
59  
60

- 1  
2  
3  
4  
5  
6 2006;2:181-189.  
7  
8  
9 22. Kim HM, Himeno T, Kawashita M, Lee JH, Kokubo T, Nakamura T. Surface  
10  
11 potential change in bioactive titanium metal during the process of apatite formation  
12  
13 in simulated body fluid. J Biomed Mater Res A. 2003;67:1305-1309.  
14  
15  
16  
17  
18 23. Takadama H, Kim HM, Kokubo T, Nakamura T. An X-ray photoelectron  
19  
20 spectroscopy study of the process of apatite formation on bioactive titanium metal.  
21  
22 J Biomed Mater Res 2001;55:185-193.  
23  
24  
25  
26  
27 24. Miyazaki T, Kim HM, Kokubo T, Ohtsuki C, Kato H, Nakamura T. Mechanism of  
28  
29 Bonelike Apatite Formation on Bioactive Tantalum Metal in Simulated Body Fluid.  
30  
31 Biomaterials 2002;23:827-832.  
32  
33  
34  
35  
36  
37 25. Takadama H, Kim HM, Kokubo T, Nakamura T. X-ray photoelectron spectroscopy  
38  
39 study on the process of apatite formation on a sodium silicate glass in simulated  
40  
41 body fluid. J Am Ceram Soc 2002;85:1933–1936.  
42  
43  
44  
45  
46  
47  
48  
49  
50  
51  
52  
53  
54  
55  
56  
57  
58  
59  
60

Table 1 Zeta potentials of the samples (N=3)

Sample	Zeta potential (mV)
HfO <sub>2</sub>	-15.5±1.79
HfTiO <sub>4</sub>	-41.9±2.05*

\* $p < 0.001$  in comparison with HfO<sub>2</sub>

For Peer Review

1  
2  
3  
4  
5  
6 **Figure captions**  
7

8  
9 **Fig. 1** XPS spectra of NaOH- and heat-treated metal substrates. This shows that surface  
10  
11  
12 OH content is different by composition of the alloy.  
13

14  
15 **Fig. 2** TF-XRD patterns of NaOH- and heat-treated metal substrates before (left) and  
16  
17  
18 after (right) immersion in SBF for 7 days. This shows that surface crystalline phase is  
19  
20  
21 significantly different by composition of the alloy.  
22

23  
24 **Fig. 3** SEM images and EDX spectra of NaOH- and heat-treated metal substrates after  
25  
26  
27 immersion in SBF for 7 days. Star marks indicate the positions of EDX analysis. Apatite  
28  
29  
30 formation was not observed for intermediate composition of Ti-60Hf.  
31

32  
33  
34 **Fig. 4** High-magnification SEM images and FT-IR ATR spectrum of the spherical  
35  
36  
37 particles formed on the surface of the treated Ti-80Hf substrate after immersion in SBF  
38  
39  
40 for 7 days. This shows that the formed apatite contains  $\text{HPO}_4^{2-}$  and  $\text{CO}_3^{2-}$ .  
41  
42  
43  
44  
45  
46  
47  
48  
49  
50  
51  
52  
53  
54  
55  
56  
57  
58  
59  
60

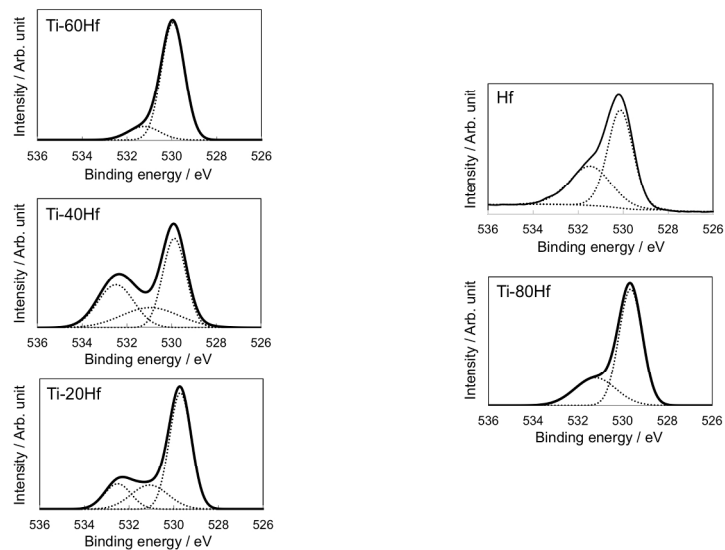


Fig. 1

Fig.1

338x190mm (180 x 180 DPI)

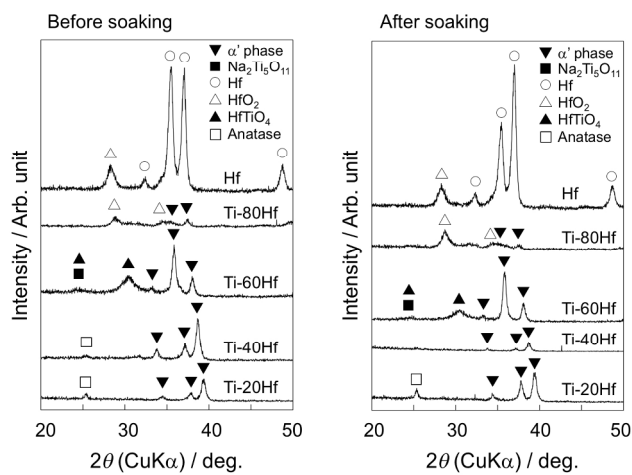


Fig. 2

Fig.2

338x190mm (180 x 180 DPI)

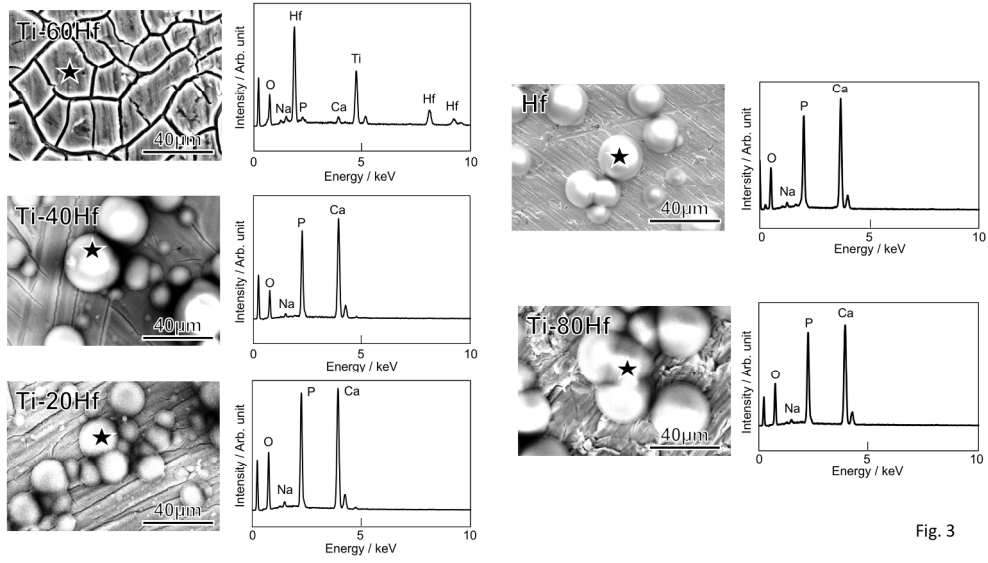


Fig. 3

Fig.3

338x190mm (180 x 180 DPI)

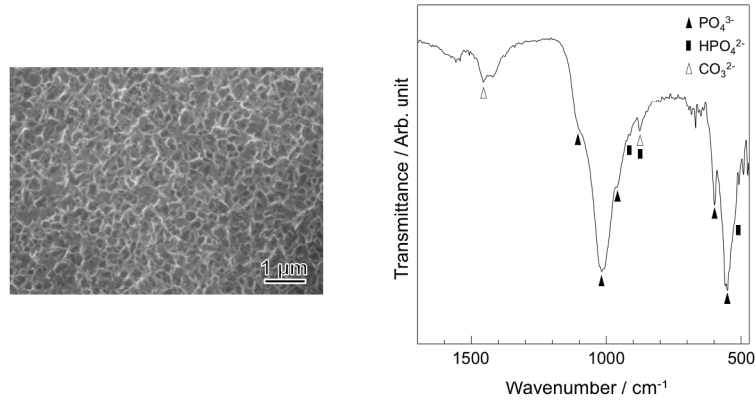


Fig. 4

Fig.4

338x190mm (180 x 180 DPI)